

Cardiac Mechanics in Heart Failure with Preserved Ejection Fraction

Karthik Seetharam¹, Partho Sengupta², and Christopher Bianco³

¹Mount Sinai Hospital

²West Virginia University School of Medicine

³West Virginia University Heart and Vascular Institute

April 28, 2020

Abstract

Heart failure with preserved ejection fraction (HFpEF) is a complex clinical entity associated with significant morbidity and mortality. Common comorbidities including hypertension, coronary artery disease, diabetes, chronic kidney disease, obesity, and increasing age predispose to preclinical diastolic dysfunction that often progresses to frank HFpEF. That said, clinical HFpEF is typically associated with some degree of diastolic dysfunction or can occur in the absence of many conventional diastolic dysfunction indices. The exact biologic links between risk factors, structural changes, and clinical manifestations are not clearly apparent. Innovative approaches including deformation imaging have enabled deeper understanding of HFpEF cardiac mechanics beyond conventional metrics. Furthermore, predictive analytics through data driven platforms have allowed for a deeper understanding of HFpEF phenotypes. This review focuses on the changes in cardiac mechanics that occur through preclinical myocardial dysfunction to clinically apparent HFpEF.

Introduction

Heart Failure with preserved ejection fraction (HFpEF) is a complex clinical entity associated with significant morbidity and mortality. HFpEF is responsible for approximately half of all heart failure hospitalizations, with mean survival similar to those with heart failure with reduced ejection fraction¹. HFpEF typically begins with risk factor exposure, which promotes abnormal cardiac mechanics and preclinical myocardial dysfunction. Preclinical diastolic dysfunction is present in approximately $\frac{1}{4}$ of the adult population². A significant proportion of patients with diastolic dysfunction go on to develop frank clinical heart failure.

The exact biologic links responsible for diastolic dysfunction and heart failure are not clearly apparent, but can be attributed to a complex interplay of various pathological conditions on background aging³. Until recently, myocardial determinants of HFpEF were thought primarily related to impairments in left ventricular relaxation and chamber stiffness. However, contemporary studies recognize the contribution of subtle left and right ventricular systolic dysfunction, as well as the impact of left atrial function and pericardial compliance. Furthermore, myocardial dysfunction may initially occur only during exercise and the static resting evaluation may not fully characterize potential dynamic changes. Therefore, assessment of cardiac mechanics during rest and exercise plays an important role in diagnosis and prognostication⁴. This review focuses on the changes in cardiac mechanics that occur through the spectrum of preclinical myocardial dysfunction into clinically apparent HFpEF.

Left Ventricular Mechanics

Each myocardial layer contributes to longitudinal, circumferential, and radial deformation. Longitudinal deformation is largely dependent on a well functioning subendocardial fiber layer, while circumferential

deformation of the left ventricle (LV) is predominately dependent on the subepicardial fiber layer⁵. LV shearing forces occur within the three-dimensional myofiber orientation causing the largest shear force in the circumferential-longitudinal plane referred to as LV twist or torsional deformation. The rotation of LV base and apex in opposite directions, combined with twist shearing forces, are responsible for translating a mere 15-20% maximal myocyte length shortening into an ultimate LV cavity volume reduction of over half. These same shear forces are responsible for untwisting during diastolic recoil. Left ventricular diastolic untwisting releases stored mechanical energy and creates a vacuum effect facilitate movement of blood from the left atrium (LA) to the LV.

The predominant myocardial mechanics of HFpEF or restrictive cardiomyopathies involve subendocardial fiber dysfunction leading to decrements in longitudinal strain. Epicardial layer derived circumferential strain and torsional shear forces remain relatively preserved or even increased to supranormal values early in the disease course⁶. These compensatory circumferential and twist mechanics allow for preservation of ejection fraction. On the other hand, constrictive pericarditis, a common HFpEF mimic, leads to a reciprocal situation of decreased circumferential and torsion forces while longitudinal forces are preserved⁷. These cardiac mechanics can serve as an adjunct to traditional echocardiographic signs differentiating features of constrictive versus restrictive physiology, as clinical presentation may be similar between disease states.

Preclinical Myocardial Dysfunction

Traditional imaging biomarkers may be normal in early subclinical disease, however reduced global longitudinal strain (GLS) related to subendocardial dysfunction is common. (Figure 1). The prevalence of reduced GLS in asymptomatic type 2 diabetes mellitus has been reported to range from 37% to 54%⁸. Impaired longitudinal strain may be present prior to the onset of LV remodeling and hypertrophy⁹. Furthermore, reduced longitudinal strain may exist despite normal or near normal conventional Doppler and tissue Doppler-derived parameters of diastolic function¹⁰(Figure 2). Compensatory subepicardial hypertrophy may develop in an effort to reduce subendocardial wall stress and preserve ejection fraction¹¹. Despite mild, resting impairment in longitudinal mechanics, those with preclinical myocardial dysfunction typically augment longitudinal strain to near normal values during exercise¹². Complex interactions between protracted risk factor exposure and progressive structural changes influence the progression from the asymptomatic phase to symptomatic heart failure. High risk structural findings in asymptomatic patients at elevated risk for progression to symptomatic disease include elevated E/e', left ventricular hypertrophy (LVH), and abnormal GLS¹².

Clinical Heart Failure

Left ventricular cardiac mechanics associated with symptomatic heart failure are complex and often counterintuitive. Several investigators have shown that impaired longitudinal strain is a frequent finding in symptomatic HFpEF patients (Figure 2) and predictive of poor outcomes^{13,14}. Although a deterioration in longitudinal mechanics is common, global circumferential strain (GCS), LV twist, and twist/untwist rates may remain normal or even increase to supranormal values⁶ early in the disease course (Figure 1). This allows for preservation of the ejection fraction via compensatory contributions from the subepicardial layer to circumferential and LV twist deformation. If subepicardial dysfunction is present and compensation is not possible, ejection fraction falls¹⁵. Circumferential and twist deformation may remain normal or increased early in the disease course. However, time to peak twist and untwist are often prolonged and signals subtle impairments of systolic and diastolic function¹⁶. Advanced HFpEF is characterized by a progressive deterioration of twist/untwist mechanics, as well as circumferential, radial, and longitudinal deformation^{17,18}.

Resting deformation can be used to predict invasive hemodynamics. In HFpEF patients, the ratio of mitral E to global longitudinal strain rate in isovolumic relaxation can predict left ventricular filling pressure¹⁹. Furthermore, the ratio of resting global circumferential strain to global longitudinal strain can serve as potential predictor of a pathologic rise in pulmonary capillary wedge pressure during exercise²⁰.

Exercise imaging for diastolic function and cardiac mechanical assessment can aid tremendously in the initial HFpEF diagnostic work-up. Recent guidelines recommend functional exercise echocardiographic stress testing

in patients at intermediate likelihood of HFpEF following an initial morphofunctional assessment²¹. Despite impaired resting longitudinal deformation, those with preclinical disease can augment longitudinal mechanics during exertion to a greater extent than those who have progressed to symptomatic heart failure. This in part explains the initial onset of exertional symptoms alone in patients transitioning from preclinical disease into frank clinical heart failure²². Furthermore, impaired GLS during exercise has been independently associated with an increased occurrence of all-cause mortality and HF hospitalizations²³.

Left Atrial Mechanics

Left atrial (LA) enlargement has long been recognized as a marker of increased cardiovascular risk²⁴. However, impaired LA phasic function evident by reduced strain occurs prior to LA enlargement and may be an early marker of risk²⁵. Thin atrial walls challenge deformation analysis, however a growing body of evidence utilizing LA strain is accumulating and recent guidelines for standardization of LA deformation have been published²⁶.

The LA functions as a reservoir for pulmonary venous return during ventricular systole, as a conduit during early ventricular filling, and as a contractile booster pump that contributes to late ventricular filling. Atrio-ventricular deformation are closely interrelated and governed by the concepts of atrioventricular coupling. Reservoir function is dependent on both on atrial volume and compliance, as well as LV systolic longitudinal annular excursion. Conduit function is dependent on the atrioventricular pressure gradient created during LV diastolic recoil. Atrial contractile function is dependent on both intrinsic pump function and late diastolic ventricular afterload.

Preclinical Myocardial Dysfunction

Preclinical LA dysfunction is characterized by reduced reservoir and conduit function while atrial contractile function remains normal²⁷ or even increased²⁸ (Figure 3). Early in the disease spectrum, compensatory enhanced LA contractile function is necessary for enhanced late LV filling. LA deformation abnormalities occur prior to clear LA anatomic remodeling. Impaired reservoir phasic performance may occur in the absence of diastolic dysfunction or ventricular remodeling²⁵. In patients with normal LA size, impaired LA reservoir function is associated with an increased risk of future heart failure hospitalization²⁹. In at risk hypertensive patients, decreased LA contractile function is strongly predictive of future adverse cardiac events and death³⁰. Furthermore, hypertension risk mitigation strategies including renin-angiotensin-aldosterone system inhibitor institution leads to improvements in LA strain³¹.

Clinical Heart Failure

A growing body of literature supports the pivotal role of LA functional failure leading to pulmonary congestion and symptom onset. Specifically, atrial contractile failure to compensate for reservoir and/or conduit dysfunction may lead to overt clinical heart failure³² (Figures 3). Atrial fibrillation leading to failure of contractile compensation, may be large determinant of symptom onset, and compensatory enhanced conduit function becomes essential in this situation. Early exercise-induced symptoms may also be related to conduit function failure in the setting of impaired reservoir function³³. Advanced symptomatic HFpEF is characterized by an eventual impairment in all three atrial functional phases³⁴ (Figures 2 and 3).

Hewing et al demonstrated that in patients with sinus rhythm, LA reservoir, conduit, and contractile function all inversely correlated with pulmonary capillary wedge pressure. However, LA contractile strain could independently predict invasively measured pulmonary capillary wedge pressure with a higher diagnostic accuracy than average E/E' ratio³⁵. Furthermore, Lundberg et al found LA strain to outperform the current guideline recommended algorithm incorporating E/e', LA volume index, and max tricuspid regurgitation velocity in determining invasively measured elevated pulmonary capillary wedge pressure³⁶.

Impaired LA reservoir strain may provide enhanced diagnostic accuracy beyond conventional echocardiographic measures to discriminate true HFpEF from non-cardiac dyspnea³⁷. Impaired resting LA reservoir strain is associated with decreased peak oxygen consumption³⁸. LA reservoir strain normally increases during exercise, but this typical exercise related augmentation is blunted in symptomatic patients. Impaired

LA reservoir augmentation with exercise leads to right ventricular-pulmonary circulation uncoupling and exercise ventilatory inefficiency³⁹. Furthermore, resting LA reservoir strain may outperformed LV GLS in its diagnostic utility and prognostic ability for prediction of heart failure hospitalization³⁸.

Right Heart Mechanics

Right heart dysfunction is common throughout the clinical progression from preclinical disease to overt heart failure (Figure 1). Almost half of patients with HFpEF have right heart dysfunction as assessed by RV longitudinal strain³⁸. HFpEF patients with prominent right heart dysfunction may represent a particularly high risk phenotype⁴⁰. Although far less data examining right heart deformation in HFpEF are currently available, recommendations for the standardization of right heart deformation imaging have been published²⁶ and future study will further our understanding of right heart dysfunction.

Intact structure, function, and geometry of the interventricular septum is of utmost importance in preserving RV function. Shearing forces of the oblique interventricular septal fibers result in systolic twisting of the base toward the apex, leading to RV longitudinal motion. Interventricular septal mechanics are normally responsible for approximately 80% of RV systolic function. Circumferential compression of the transversely oriented fibers of the RV free wall result in a bellows motion, which normally contributes approximately 20% of RV systolic function^{41,42}. RV dysfunction initially involves reduced longitudinal performance with a compensatory increase in circumferential motion, therefore RV longitudinal strain may serve as a sensitive tool for identifying early dysfunction.

Asymptomatic patients with metabolic disease commonly exhibit mild reductions in RV longitudinal strain^{43,44}. With disease progression into symptomatic heart failure, almost half of HFpEF patients have RV dysfunction by deformation indices³⁸(Figure 2). RV longitudinal strain and global longitudinal early-diastolic strain rate (RV-SRe) are both more significantly impaired in patients with symptoms than in those with preclinical disease⁴⁵. Right heart dysfunction may occur as a result of resting pulmonary hypertension or exercise-induced pulmonary hypertension. However, in some patients LV GLS may be a more important predictor of impaired RV longitudinal function than pulmonary arterial systolic pressure⁴⁵, suggesting a global myocardial process as the driver of dysfunction as opposed to pulmonary hypertension alone. Nonetheless, indices incorporating simultaneous RV function and afterload provide a measure of RV performance and pulmonary circulation coupling. Among patients with HFpEF, the ratio of RV longitudinal strain to pulmonary artery systolic pressure independently predicted the composite endpoint of all-cause death and HF hospitalization, even after multivariate adjustment⁴⁶.

Impairment of right atrial deformation has also been appreciated in HFpEF patients⁴⁷. Pulmonary hypertension is associated with a decrement in right atrial strain⁴⁸. Right atrial mechanics may prove an indicator of systemic venous congestion and related cardiorenal dysfunction. A distinct HFpEF phenogroup characterized by extensive cardiac remodeling with prominent pulmonary hypertension and right heart failure exists⁴⁰. This phenogroup more often includes elderly patients with chronic kidney disease and appears to be at particularly high risk.

Potential of Machine Learning

HFpEF is heterogeneous entity affected by multiple clinical variables and structural alterations. Current methods resort to an oversimplified approach for assessment and risk stratification⁴. This one size fits all approach has not proved applicable in clinical practice. With the evolution of technology and computer capabilities, artificial intelligence (AI) is opening new frontiers in cardiovascular imaging. Machine learning (ML), a subset of AI, is ushering a new era in cardiovascular imaging by expanding boundaries not limited by conventional statistics⁴⁹. Unlike traditional approaches, ML can decipher hidden patterns and extrapolate hidden patterns within vast data matrices^{50,51}. This technology can integrate diastolic indices and speckle tracking echocardiography to offer innovative insights into HFpEF⁵² (Figure 4).

Lancaster et al performed an unsupervised, hierarchical cluster analysis of 866 patients with diastolic dysfunction graded using contemporary ASE recommendations⁵³. Major adverse cardiovascular events, hospi-

talization, and mortality were compared between conventional and cluster-based categorizations. Survival analyses of patients assessed by clustering algorithms showed improved prediction of event-free survival by cluster analysis over diastolic grade classifications for all-cause mortality and cardiac mortality.

Omar et al performed a cluster analysis of LA and LV mechanical deformation parameters that resulted in a Doppler-independent phenotypic characterization of diastolic function and provided a noninvasive estimation of LV filling pressures⁵⁴. Speckle tracking features independently clustered patients into three groups with conventional parameters verifying increasing severity of dysfunction and LV filling pressure. Subsequent investigations from the same group lead to a refined ML model for assessing LV filling pressure using fourteen speckle tracking variables⁵⁵. This model correctly identified 80% of patients with pulmonary capillary wedge pressure [?]18 mm Hg,

ML has also been applied to resting and stress deformation imaging. Tabassian et al explored the role of ML in analyzing LV long axis mechanics during stress and rest in 100 patients including those with HFpEF and healthy, hypertensive, and breathless control subjects⁵⁶. A ML algorithm was used to model spatiotemporal patterns of the speckle tracking traces and compare the ML algorithm predictions with the clinical diagnoses. The ML algorithm predicted symptoms with a high degree of accuracy and assigning subjects into four phenotypic groups. ML incorporating strain rate, compared with standard measurements, provided the greatest improvement in accuracy for predicting symptoms and 6-min walk distance. Sanchez-Martinez et al also utilized measurements of LV deformation at rest and exercise to examine differences between HFpEF and healthy patients from the MEDIA study (MEtabolic road to DIAstolic heart failure)⁵⁷. LV long-axis myocardial velocity patterns analyzed using an unsupervised ML algorithm identified a continuum from health to disease, including a transition zone associated with an uncertain diagnosis. As we move forward in the current era of cardiovascular imaging, ML algorithms will be increasingly integrated into clinical practice and cardiovascular research. These methods may help detect previously unrecognized phenotypes and tailor individualized therapies⁴.

Conclusion

HFpEF is a complex clinical entity mediated by multiple clinical factors leading to various structural alterations. Risk factor exposure leads to an evolution of abnormal myocardial mechanics in each cardiac chamber. Initially, many deformation parameters only deteriorate during exercise. Although common mechanical changes are often present, significant heterogeneity in structure and function may exist. In addition to multiple imaging biomarkers, heterogeneity of clinical features and associated medical conditions compound this syndromes complexity. Current methods resort to an oversimplified approach for assessment and risk stratification. With the evolution of technology and computer capabilities, artificial intelligence (AI) is opening new frontiers in cardiovascular imaging. This technology can be integrated with diastolic indices and speckle tracking echocardiography to offer innovative insights into HFpEF⁵².

References

1. Shah KS, Xu H, Matsouaka RA, et al. Heart Failure With Preserved, Borderline, and Reduced Ejection Fraction: 5-Year Outcomes. *J Am Coll Cardiol.* 2017;70(20):2476-2486 DOI:10.1016/j.jacc.2017.08.074. PubMed PMID: 29141781.
2. Wan SH, Vogel MW, Chen HH. Pre-clinical diastolic dysfunction. *J Am Coll Cardiol.* 2014;63(5):407-416 DOI:10.1016/j.jacc.2013.10.063. PubMed PMID: 24291270.
3. Lee DS, Gona P, Vasan RS, et al. Relation of disease pathogenesis and risk factors to heart failure with preserved or reduced ejection fraction: insights from the framingham heart study of the national heart, lung, and blood institute. *Circulation.*2009;119(24):3070-3077 DOI:10.1161/circulationaha.108.815944. PubMed PMID: 19506115.
4. Bianco CM, Farjo PD, Ghaffar YA, Sengupta PP. Myocardial Mechanics in Patients With Normal LVEF and Diastolic Dysfunction. *JACC Cardiovasc Imaging.* 2020;13(1 Pt 2):258-271 DOI:10.1016/j.jcmg.2018.12.035. PubMed PMID: 31202770.

5. Sengupta PP, Tajik AJ, Chandrasekaran K, Khandheria BK. Twist mechanics of the left ventricle: principles and application. *JACC Cardiovasc Imaging*. 2008;1(3):366-376 DOI:10.1016/j.jcmg.2008.02.006. PubMed PMID: 19356451.
6. Wang J, Khoury DS, Yue Y, Torre-Amione G, Nagueh SF. Preserved left ventricular twist and circumferential deformation, but depressed longitudinal and radial deformation in patients with diastolic heart failure. *Eur Heart J*. 2008;29(10):1283-1289 DOI:10.1093/eurheartj/ehn141. PubMed PMID: 18385117.
7. Sengupta PP, Krishnamoorthy VK, Abhayaratna WP, et al. Disparate patterns of left ventricular mechanics differentiate constrictive pericarditis from restrictive cardiomyopathy. *JACC: Cardiovascular imaging*. 2008;1(1):29-38.
8. Wang Y, Marwick TH. Update on Echocardiographic Assessment in Diabetes Mellitus. *Curr Cardiol Rep*. 2016;18(9):85 DOI:10.1007/s11886-016-0759-0. PubMed PMID: 27443381.
9. Szelenyi Z, Fazakas A, Szenasi G, et al. The mechanism of reduced longitudinal left ventricular systolic function in hypertensive patients with normal ejection fraction. *Journal of hypertension*.2015;33(9):1962-1969.
10. Ernande L, Bergerot C, Rietzschel ER, et al. Diastolic dysfunction in patients with type 2 diabetes mellitus: is it really the first marker of diabetic cardiomyopathy? *J Am Soc Echocardiogr*.2011;24(11):1268-1275.e1261 DOI:10.1016/j.echo.2011.07.017. PubMed PMID: 21907542.
11. Zhang J. Myocardial energetics in cardiac hypertrophy. *Clin Exp Pharmacol Physiol*. 2002;29(4):351-359 DOI:10.1046/j.1440-1681.2002.03657.x. PubMed PMID: 11985549.
12. Kosmala W, Marwick TH. Asymptomatic Left Ventricular Diastolic Dysfunction: Predicting Progression to Symptomatic Heart Failure.*JACC Cardiovasc Imaging*. 2020;13(1 Pt 2):215-227 DOI:10.1016/j.jcmg.2018.10.039. PubMed PMID: 31005530.
13. Shah AM, Claggett B, Sweitzer NK, et al. Prognostic Importance of Impaired Systolic Function in Heart Failure With Preserved Ejection Fraction and the Impact of Spironolactone. *Circulation*.2015;132(5):402-414 DOI:10.1161/circulationaha.115.015884. PubMed PMID: 26130119.
14. Morris DA, Ma XX, Belyavskiy E, et al. Left ventricular longitudinal systolic function analysed by 2D speckle-tracking echocardiography in heart failure with preserved ejection fraction: a meta-analysis.*Open Heart*. 2017;4(2):e000630 DOI:10.1136/openhrt-2017-000630. PubMed PMID: 29018535.
15. Sengupta PP, Narula J. Reclassifying heart failure: predominantly subendocardial, subepicardial, and transmural. *Heart Fail Clin*.2008;4(3):379-382 DOI:10.1016/j.hfc.2008.03.013. PubMed PMID: 18598989.
16. Stohr EJ, Shave RE, Baggish AL, Weiner RB. Left ventricular twist mechanics in the context of normal physiology and cardiovascular disease: a review of studies using speckle tracking echocardiography.*Am J Physiol Heart Circ Physiol*. 2016;311(3):H633-644 DOI:10.1152/ajpheart.00104.2016. PubMed PMID: 27402663.
17. Yip GW, Zhang Q, Xie JM, et al. Resting global and regional left ventricular contractility in patients with heart failure and normal ejection fraction: insights from speckle-tracking echocardiography.*Heart*. 2011;97(4):287-294 DOI:10.1136/hrt.2010.205815. PubMed PMID: 21193686.
18. Nguyen JS, Lakkis NM, Bobek J, Goswami R, Dokainish H. Systolic and diastolic myocardial mechanics in patients with cardiac disease and preserved ejection fraction: impact of left ventricular filling pressure. *J Am Soc Echocardiogr*. 2010;23(12):1273-1280 DOI:10.1016/j.echo.2010.09.008. PubMed PMID: 20970305.
19. Hatipoglu S, Ozdemir N, Babur Guler G, et al. Prediction of elevated left ventricular filling pressures in patients with preserved ejection fraction using longitudinal deformation indices of the left ventricle.*Eur Heart J Cardiovasc Imaging*. 2015;16(10):1154-1161 DOI:10.1093/ehjci/jev063. PubMed PMID: 25896356.

20. Biering-Sorensen T, Santos M, Rivero J, et al. Left ventricular deformation at rest predicts exercise-induced elevation in pulmonary artery wedge pressure in patients with unexplained dyspnoea. *Eur J Heart Fail.* 2017;19(1):101-110 DOI:10.1002/ejhf.659. PubMed PMID: 27878925.
21. Pieske B, Tschope C, de Boer RA, et al. How to diagnose heart failure with preserved ejection fraction: the HFA-PEFF diagnostic algorithm: a consensus recommendation from the Heart Failure Association (HFA) of the European Society of Cardiology (ESC). *Eur Heart J.* 2019;40(40):3297-3317 DOI:10.1093/eurheartj/ehz641. PubMed PMID: 31504452.
22. Kosmala W, Rojek A, Przewlocka-Kosmala M, Mysiak A, Karolko B, Marwick TH. Contributions of Nondiastolic Factors to Exercise Intolerance in Heart Failure With Preserved Ejection Fraction. *J Am Coll Cardiol.* 2016;67(6):659-670 DOI:10.1016/j.jacc.2015.10.096. PubMed PMID: 26868691.
23. Wang J, Fang F, Wai-Kwok Yip G, et al. Left ventricular long-axis performance during exercise is an important prognosticator in patients with heart failure and preserved ejection fraction. *Int J Cardiol.* 2015;178:131-135 DOI:10.1016/j.ijcard.2014.10.130. PubMed PMID: 25464236.
24. Tsang TS, Barnes ME, Gersh BJ, Bailey KR, Seward JB. Left atrial volume as a morphophysiologic expression of left ventricular diastolic dysfunction and relation to cardiovascular risk burden. *The American journal of cardiology.* 2002;90(12):1284-1289.
25. Cameli M, Lisi M, Righini FM, et al. Left atrial strain in patients with arterial hypertension. Paper presented at: International Cardiovascular Forum Journal2013.
26. Badano LP, Koliass TJ, Muraru D, et al. Standardization of left atrial, right ventricular, and right atrial deformation imaging using two-dimensional speckle tracking echocardiography: a consensus document of the EACVI/ASE/Industry Task Force to standardize deformation imaging. *European Heart Journal-Cardiovascular Imaging.* 2018;19(6):591-600.
27. Fang NN, Sui DX, Yu JG, et al. Strain/strain rate imaging of impaired left atrial function in patients with metabolic syndrome. *Hypertens Res.* 2015;38(11):758-764 DOI:10.1038/hr.2015.76. PubMed PMID: 26178155.
28. Brecht A, Oertelt-Prigione S, Seeland U, et al. Left Atrial Function in Preclinical Diastolic Dysfunction: Two-Dimensional Speckle-Tracking Echocardiography-Derived Results from the BEFRI Trial. *J Am Soc Echocardiogr.* 2016;29(8):750-758 DOI:10.1016/j.echo.2016.03.013. PubMed PMID: 27156904.
29. Morris DA, Belyavskiy E, Aravind-Kumar R, et al. Potential Usefulness and Clinical Relevance of Adding Left Atrial Strain to Left Atrial Volume Index in the Detection of Left Ventricular Diastolic Dysfunction. *JACC Cardiovasc Imaging.* 2018;11(10):1405-1415 DOI:10.1016/j.jcmg.2017.07.029. PubMed PMID: 29153567.
30. Kaminski M, Steel K, Jerosch-Herold M, et al. Strong cardiovascular prognostic implication of quantitative left atrial contractile function assessed by cardiac magnetic resonance imaging in patients with chronic hypertension. *Journal of Cardiovascular Magnetic Resonance.* 2011;13(1):42.
31. Dimitroula H, Damvopoulou E, Giannakoulas G, et al. Effects of renin-angiotensin system inhibition on left atrial function of hypertensive patients: an echocardiographic tissue deformation imaging study. *American journal of hypertension.* 2010;23(5):556-561.
32. Sanchis L, Gabrielli L, Andrea R, et al. Left atrial dysfunction relates to symptom onset in patients with heart failure and preserved left ventricular ejection fraction. *Eur Heart J Cardiovasc Imaging.* 2015;16(1):62-67 DOI:10.1093/ehjci/jeu165. PubMed PMID: 25187609.
33. von Roeder M, Rommel K-P, Kowallick JT, et al. Influence of left atrial function on exercise capacity and left ventricular function in patients with heart failure and preserved ejection fraction. *Circulation: Cardiovascular Imaging.* 2017;10(4):e005467.

34. Santos AB, Kraigher-Krainer E, Gupta DK, et al. Impaired left atrial function in heart failure with preserved ejection fraction. *European journal of heart failure*. 2014;16(10):1096-1103.
35. Hewing B, Theres L, Spethmann S, Stangl K, Dreger H, Knebel F. Left atrial strain predicts hemodynamic parameters in cardiovascular patients. *Echocardiography*. 2017;34(8):1170-1178.
36. Lundberg A, Johnson J, Hage C, et al. Left atrial strain improves estimation of filling pressures in heart failure: a simultaneous echocardiographic and invasive haemodynamic study. *Clinical Research in Cardiology*. 2019;108(6):703-715.
37. Reddy YNV, Obokata M, Egbe A, et al. Left atrial strain and compliance in the diagnostic evaluation of heart failure with preserved ejection fraction. *Eur J Heart Fail*. 2019;21(7):891-900 DOI:10.1002/ejhf.1464. PubMed PMID: 30919562.
38. Freed BH, Daruwalla V, Cheng JY, et al. Prognostic Utility and Clinical Significance of Cardiac Mechanics in Heart Failure With Preserved Ejection Fraction: Importance of Left Atrial Strain. *Circ Cardiovasc Imaging*. 2016;9(3) DOI:10.1161/circimaging.115.003754. PubMed PMID: 26941415.
39. Sugimoto T, Bandera F, Generati G, Alfonzetti E, Bussadori C, Guazzi M. Left Atrial Function Dynamics During Exercise in Heart Failure: Pathophysiological Implications on the Right Heart and Exercise Ventilation Inefficiency. *JACC Cardiovasc Imaging*. 2017;10(10 Pt B):1253-1264 DOI:10.1016/j.jcmg.2016.09.021. PubMed PMID: 28017395.
40. Shah SJ, Katz DH, Selvaraj S, et al. Phenomapping for novel classification of heart failure with preserved ejection fraction. *Circulation*. 2015;131(3):269-279 DOI:10.1161/circulationaha.114.010637. PubMed PMID: 25398313.
41. Buckberg G, Hoffman JI, Nanda NC, Coghlan C, Saleh S, Athanasuleas C. Ventricular torsion and untwisting: further insights into mechanics and timing interdependence: a viewpoint. *Echocardiography*. 2011;28(7):782-804.
42. Buckberg G, Hoffman JI. Right ventricular architecture responsible for mechanical performance: unifying role of ventricular septum. *The Journal of thoracic and cardiovascular surgery*. 2014;148(6):3166-3171. e3164.
43. Kosmala W, Przewlocka-Kosmala M, Mazurek W. Subclinical right ventricular dysfunction in diabetes mellitus—an ultrasonic strain/strain rate study. *Diabet Med*. 2007;24(6):656-663 DOI:10.1111/j.1464-5491.2007.02101.x. PubMed PMID: 17367309.
44. Wong CY, O'Moore-Sullivan T, Leano R, Hukins C, Jenkins C, Marwick TH. Association of subclinical right ventricular dysfunction with obesity. *Journal of the American College of Cardiology*. 2006;47(3):611-616.
45. Morris DA, Gailani M, Vaz Perez A, et al. Right ventricular myocardial systolic and diastolic dysfunction in heart failure with normal left ventricular ejection fraction. *J Am Soc Echocardiogr*. 2011;24(8):886-897 DOI:10.1016/j.echo.2011.04.005. PubMed PMID: 21601421.
46. Bosch L, Lam CSP, Gong L, et al. Right ventricular dysfunction in left-sided heart failure with preserved versus reduced ejection fraction. *Eur J Heart Fail*. 2017;19(12):1664-1671 DOI:10.1002/ejhf.873. PubMed PMID: 28597497.
47. Jain S, Kuriakose D, Edelstein I, et al. Right atrial phasic function in heart failure with preserved and reduced ejection fraction. *JACC: Cardiovascular Imaging*. 2019;12(8 Part 1):1460-1470.
48. Deschle HA, Amenabar A, Casso NA, et al. Behavior of right atrial strain in high systolic pulmonary artery pressure. *Echocardiography*. 2018;35(10):1557-1563.
49. Seetharam K, Shrestha S, Mills JD, Sengupta PP. Artificial Intelligence in Nuclear Cardiology: Adding Value to Prognostication. *Current Cardiovascular Imaging Reports*. 2019;12(5) DOI:10.1007/s12410-019-9490-8.

50. Seetharam K, Kagiya N, Sengupta PP. Application of mobile health, telemedicine and artificial intelligence to echocardiography. *Echo Res Pract.* 2019;6(2):R41-R52 DOI:10.1530/ERP-18-0081. PubMed PMID: 30844756.
51. Seetharam K, Shrestha S, Sengupta P. Artificial Intelligence in Cardiac Imaging. *US Cardiology Review.* 2020;13:110-116 DOI:10.15420/usc.2019.19.2.
52. Narula J. Are we up to speed?: from big data to rich insights in CV imaging for a hyperconnected world. *JACC Cardiovasc Imaging.*2013;6(11):1222-1224 DOI:10.1016/j.jcmg.2013.09.007. PubMed PMID: 24229779.
53. Lancaster MC, Salem Omar AM, Narula S, Kulkarni H, Narula J, Sengupta PP. Phenotypic Clustering of Left Ventricular Diastolic Function Parameters: Patterns and Prognostic Relevance. *JACC Cardiovasc Imaging.* 2019;12(7 Pt 1):1149-1161 DOI:10.1016/j.jcmg.2018.02.005. PubMed PMID: 29680357.
54. Omar AMS, Narula S, Abdel Rahman MA, et al. Precision Phenotyping in Heart Failure and Pattern Clustering of Ultrasound Data for the Assessment of Diastolic Dysfunction. *JACC Cardiovasc Imaging.*2017;10(11):1291-1303 DOI:10.1016/j.jcmg.2016.10.012. PubMed PMID: 28109936.
55. Salem Omar AM, Shameer K, Narula S, et al. Artificial Intelligence-Based Assessment of Left Ventricular Filling Pressures From 2-Dimensional Cardiac Ultrasound Images. *JACC Cardiovasc Imaging.*2018;11(3):509-510 DOI:10.1016/j.jcmg.2017.05.003. PubMed PMID: 28734920.
56. Tabassian M, Sunderji I, Erdei T, et al. Diagnosis of Heart Failure With Preserved Ejection Fraction: Machine Learning of Spatiotemporal Variations in Left Ventricular Deformation. *J Am Soc Echocardiogr.* 2018;31(12):1272-1284.e1279 DOI:10.1016/j.echo.2018.07.013. PubMed PMID: 30146187.
57. Sanchez-Martinez S, Duchateau N, Erdei T, et al. Machine Learning Analysis of Left Ventricular Function to Characterize Heart Failure With Preserved Ejection Fraction. *Circ Cardiovasc Imaging.*2018;11(4):e007138 DOI:10.1161/circimaging.117.007138. PubMed PMID: 29661795.

Figure 1 Temporal Evolution of Myocardial Mechanics

*modified from Bianco et al. *J Am Coll Cardiol Img* 2020;13:258–71

LV = left ventricular, LA = left atrial, RV = right ventricular

Figure 2 Parameters of Myocardial Mechanics in HFpEF

A. Impairment of left ventricular global longitudinal strain and mechanical dispersion are common HFpEF mechanical changes. B. Reductions in left atrial reservoir, conduit, and contractile function commonly encountered in symptomatic HFpEF. C. HFpEF associated impairment of right ventricular free wall and four chamber deformation. D. Despite normal or near normal tissue Doppler-derived parameters of diastolic function, significant deteriorations of mechanical deformation may exist. $GSL_Endo_Peak_Avg$ = Peak endocardial global longitudinal strain average, $LASr_ED$ = Left atrial reservoir strain at end-diastole, $LAScd_ED$ = Left atrial conduit strain at end-diastole, $LAct_ED$ = Left atrial contractile strain at end-diastole, $RVFWSL$ = Right ventricular free wall longitudinal strain, $RV4CSL$ = Right ventricular 4 chamber longitudinal strain

Figure 3 Temporal Evolution of Left Atrial Failure

Preclinical dysfunction is associated with a reduction in reservoir and conduit function, while relative contractile function remains normal or increased. Atrial contractile failure, along with further reductions in reservoir and conduit function, are associated with symptom onset. Advanced symptomatic HFpEF is characterized by an eventual decrement in all 3 atrial strain phases.

Figure 4 Clustering Dendrograms for Conventional Variables and Their STE Correspondents

*reprinted with permission from ⁵⁴ Omar et al *J Am Coll Cardiol Img.*2017;10(11):1291-1303

Clustering dendrograms using STE and conventional variables together. The dissimilarity matrix is given as a heat map of Euclidean distance (red). The AU (red numbers) and BP (green numbers) were calculated. AU values are shown only for leaflets that had an AU>95% (considered statistically significant). Significant proximity of variables in the clustering leaflets were decided using 2D-LAVmax, E/e', A-wave velocity, and a' velocity were shown to be in perfect proximity with their STE counterparts STE-LAV max, VR-E/SR-E_{AV}, VR-A_{AV}, and SR-A_{AV}, respectively (AU = 97%, 96%, 98%, and 100%, respectively). The conventional parameters e'/a' and E/A were also in significant proximity to their STE counterparts SR-E/SR-A_{AV} and VR-E/VR-A_{AV}, respectively (AU = 98%) and also between e' and s' and their STE counterparts SR-E_{AV} and SR-S_{AV}, respectively (AU = 100%). STE = speckle tracking echocardiogram, E = pulsed Doppler derived mitral flow early diastolic velocity; E' = tissue Doppler derived mitral annular early diastolic velocity; E/A = Doppler derived mitral flow early to late diastolic velocity ratio; E/e' = ratio of Doppler derived mitral flow early diastolic velocity to tissue Doppler derived mitral annular early diastolic velocity; LAV = left atrial maximum volume; AU = approximately unbiased probability; 2D = 2-dimensional; VR-E = rate of volume expansion at early diastole, SR-A_{AV} = peak atrioventricular strain rate during atrial contraction; SR-E_{AV} = early diastolic peak atrioventricular strain rate; SRE/SRA_{AV} = ratio between atrioventricular strain rate at early diastole and during atrial contraction; TLVd = total left heart volume during ventricular diastole; TLVs = total left heart volume during ventricular systole; VR-A_{AV} = peak atrioventricular volume expansion rate at left atrial contraction; VR-E_{AV} = early diastolic peak atrioventricular volume expansion rate; VRE/SRE_{AV} = ratio between atrioventricular volume expansion rate and strain rate at early diastole; VRE-VRA_{AV} = ratio between atrioventricular volume expansion rate at early diastole and during atrial contraction.

Figure 1 Temporal Evolution of Myocardial Mechanics

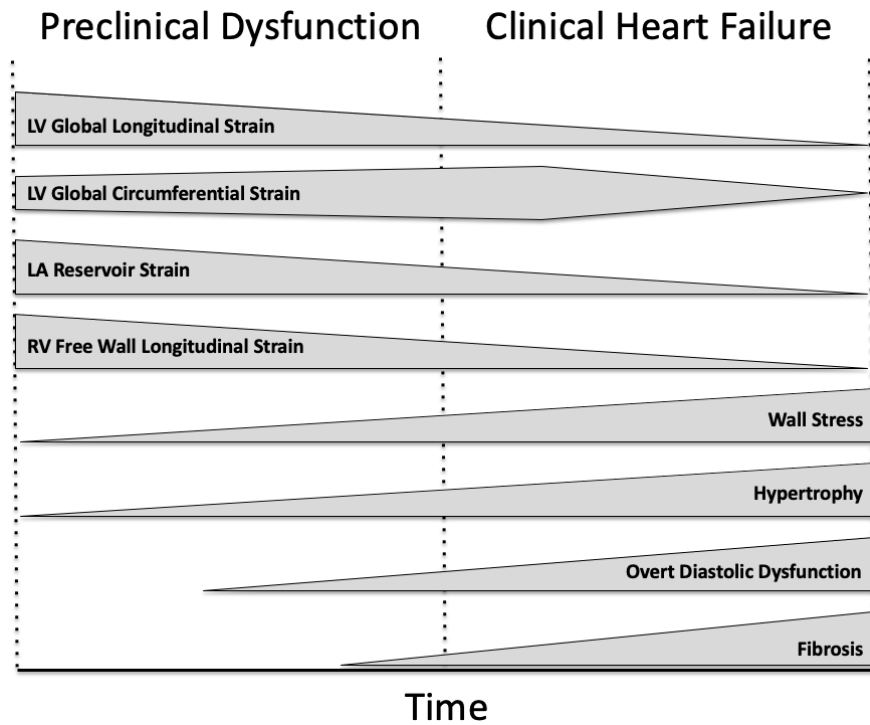


Figure 2 Parameters of Myocardial Mechanics in HFpEF

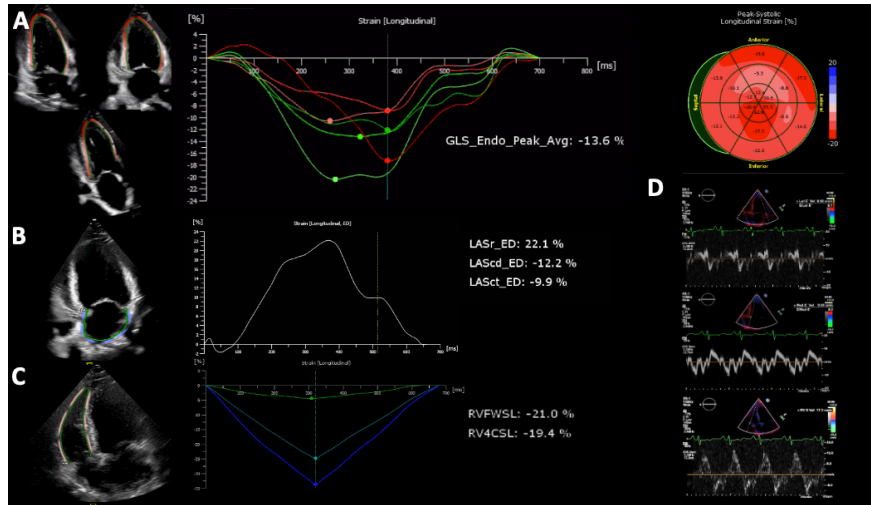


Figure 3 Temporal Evolution of Left Atrial Failure

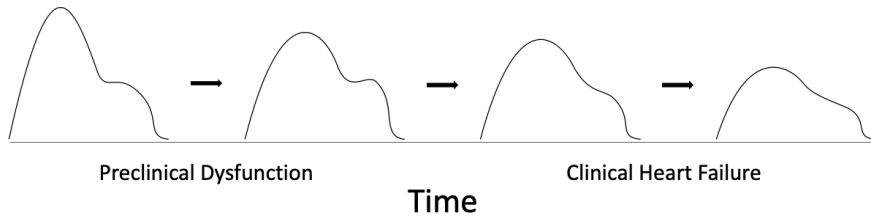


Figure 4 Clustering Dendrograms for conventional variables and their Speckle Tracking Correspondents

